RSC Advances

PAPER

View Article Online
View Journal | View Issue

Cite this: *RSC Adv.*, 2021, **11**, 39838

Assessment and treatment of floodwater in the Vietnamese Mekong Delta using a simple filter system based on silver nanoparticles coated onto activated carbon derived from rice husk†

My Uyen Dao,[ab] Hien Y Hoang, *[c] Anh Khoa Tran[c] and Hong Hanh Cong[d]

The floods in the Vietnamese Mekong Delta have long caused a shortage of clean water supply, which has a significant impact on the indigenous people in the region. We have conducted a preliminary survey of the water quality of the Hau Giang River (one of the two main branches of the Mekong River) before, during, and after the flood season. The obtained results demonstrated that the water in the Hau Giang River was highly turbid and contaminated with a large number of harmful microorganisms. Thus, in this study, a simple filter system based on silver nanoparticles coated onto activated carbon derived from rice husk (AgNPs@AC) has been proposed for treating floodwater from the Hau Giang River. The optimal conditions for AgNPs@AC preparation were established. The prepared AgNPs@AC was then characterized using various surface analyses such as SEM, TEM, XRD, BET, FTIR, and DLS. The initial floodwater source would be pre-treated with polyaluminum chloride using the coagulation–sedimentation method to remove the suspended solids before being discharged into the filtration column containing AgNPs@AC. The results showed that the filter system based on AgNPs@AC performed well in removing turbidity, dissolved solids, suspended solids, color, and bacteria from the floodwater. In addition, it was determined that the filter column with a 30 mm thick AgNPs@AC layer could continuously process 1300 m^3 of the floodwater and had a service life of more than two months. The findings of this study not only added to our understanding of the floodwater treatment capacity of activated carbon coated nanoparticles, but they also provided valuable information for water treatment plants along the Hau Giang River, aquatic ecosystem researchers, and public health researchers.

Received 7th September 2021
Accepted 3rd December 2021

DOI: 10.1039/d1ra06722b

rsc.li/rsc-advances

Introduction

In recent years, global climate change has already resulted in severe consequences, particularly widespread floods with increasing frequency, scale, and intensity, causing large-scale flooding phenomena in the low-lying delta. Most areas of the Vietnamese Mekong Delta benefit from their location in the lower reaches of the Mekong River Delta, but they also face many challenges from inundation. Along with giving sediment to grow agricultural businesses in delta areas, the seasonal flood, which lasts from 4–5 months per year, has also produced cleansing water scarcity in production and daily living.[1] During the flood season, the landfills are flooded to depths of 0.5 to 1.2 meters, causing organic waste, human excrement, and dead animals to mix with the water and flow into the rivers. Furthermore, heavy rain brings a large amount of trash from industrial plants, agricultural production, and a large amount of leftover food from fish rafts in the upstream areas, resulting in water pollution in the downstream areas. Permanent use of polluted floodwater can endanger human health risks by causing outbreaks of several epidemic diseases such as cholera, diarrhea, and dengue fever, infectious diseases, gastritis-related diseases, poisoning, and respiratory infections.[2,3] This is also the major cause of death for people who live in these areas. As a result, treating floodwater before being used not only solves the problem of a lack of clean water for people, but also protects their health.

Therefore, in this study, we surveyed the pollution status of floodwater in eight regions of the Vietnamese Mekong Delta along the Hau Giang River, which is one of the two main branches of the Mekong River. In particular, the water quality indicators including pH, turbidity, total dissolved solids (TDS), suspended solids (SS), color, total coliform, and fecal coliform

[a]*Center for Advanced Chemistry, Institute of Research & Development, Duy Tan University, Danang, 550000, Vietnam*
[b]*Faculty of Natural Sciences, Duy Tan University, Danang, 550000, Vietnam*
[c]*Faculty of Environment, Ho Chi Minh City University of Natural Resources and Environment, Ho Chi Minh City, 70000, Vietnam. E-mail: hhy@hcmunre.edu.vn*
[d]*Institute of Materials Science, Vietnam Academy of Science and Technology, Hanoi, 10072, Vietnam*

† Electronic supplementary information (ESI) available: Tables S1, S2 and Fig. S1–S5. See DOI: 10.1039/d1ra06722b

of floodwater were surveyed before, during, and after the inundation (corresponding to July, September, and October of 2020) to determine the pollution status of floodwater. Since then, based on the results obtained from the water quality analysis, a water treatment system has been proposed to treat domestic water in flooded areas. Furthermore, this system was designed with several criteria in mind, including simplicity, efficiency, ease of operation, and suitability to local economic conditions.

Activated carbon (AC) has long been considered to be an excellent material for treating polluted water. AC adsorbs contaminants in water favourably due to its physicochemical properties, such as the large specific surface area, highly developed porosity, and abundant functional groups on the surface. Recently, the development of AC from agricultural waste and biomass including coconut shell,[3] tabah bamboo,[4] banana peel,[5] spent coffee grounds,[6] Baobab fruit shell,[7] *Thuja occidentalis* leaves,[8] *Litsea glutinosa* seeds[9,10] have received increasing attention. Therefore, the utilization of the rice husk waste in the great granary of the Vietnamese Mekong Delta as the precursor for AC synthesis both brings high economic value and solves environmental problems. This solution will address the problem of solid waste pollution caused by rice husk in agricultural countries such as Vietnam. In fact, AC made from rice husk exhibits high effectiveness in the treatment of not only organic compounds,[11–13] but also heavy metals.[14,15]

As mentioned above, floodwater is a suitable residence for microorganisms, particularly disease bacteria. In addition to the pollutants and organic substances, the ingredient of harmful microorganisms in floodwater is necessary for treatment. Meanwhile, previous studies in medicine have shown that silver nanoparticles (AgNPs) have potent antimicrobial activity.[16,17] The AgNPs easily contact the cell membrane and penetrate inside microorganisms, where they inhibit the enzymatic system of the respiratory chain as well as alter the DNA synthesis of bacteria.[18,19] Loading AgNPs onto AC, fortunately, does not reduce the antibacterial properties of AgNPs, but on the contrary, improves water treatment performance.[20] Therefore, the goal of this study is to develop a simple filter system based on AgNPs@AC derived from rice husk that achieves high efficiency in eliminating pollutants and microorganisms while being easily assembled for large-scale applications with low cost.

Experimental

Materials

Unless otherwise specified, all reagents used in our experiments were purchased from commercial sources and used exactly as received. Silver nitrate ($AgNO_3$, ≥99.8%) of reagent grade was purchased from Merck (Germany). Sodium citrate ($C_6H_5O_7Na_3$, 99%) and sodium hydroxide (NaOH, ≥99.5%) were commercial products from Sigma-Aldrich. Polyaluminium chloride and kali alum for coagulation–sedimentation studies were obtained from Vikram PAC, India. Quartz sand as a filter support material was obtained from Vietnam.

All the glassware before being used in experiments was rinsed thoroughly with deionized water and dried up to avoid any coagulation caused by electrolytes. Rice husk was provided by a rice mill located in An Giang Province of the Mekong Delta. According to the analysis results, the elemental content of such rice husk was C 38.92%, H 4.9%, N 2.24%, O 27.12%, humility 11.5%, and ash 12%. The floodwater investigated in this study was predominantly taken from eight different locations along the Hau Giang River in three provinces of the Vietnamese Mekong Delta.

Preparation of AC derived from rice husk

The collected rice husk after being washed many times by distilled water to remove all the dust and dirt was dried at 105 °C for 10 hours. The freshly obtained rice husk was then carbonized for 60 min at the temperature of 400–600 °C with a heating speed of 10 °C min^{-1}. To prevent air from entering the furnace, into which a nitrogen stream is continuously injected at a flow rate of 25 L h^{-1} during the carbonization process. Following that, the sample was activated for 30 min by a carbon dioxide stream with a flow rate of 25 L h^{-1} at the temperature ranging from 700 °C to 900 °C. The resulting AC was crushed, washed with distilled water until pH ≈ 7, and then recovered through filtration. The filtered black powder was dried for 12 hours at 105 °C.

Preparation of AgNPs

Due to its ease of operation and high reliability, chemical synthesis methods have been commonly applied in the synthesis of metallic nanoparticles as a colloidal dispersion in aqueous solution by reducing their metal salts.[21–23] AgNPs used for floodwater treatment in the Mekong Delta were prepared by reducing sodium citrate ($C_6H_5O_7Na_3$, 99%) in silver nitrate solution ($AgNO_3$, 99%). The synthesis reaction is as follows:

$$4Ag^+ + C_6H_5O_7Na_3 + 2H_2O \rightarrow 4Ag^0 + C_6H_5O_7H_3 + 3Na^+ + H^+ + O_2$$

The AgNPs preparation was implemented under atmospheric conditions inside a 1000 mL cylindrical glass reactor with a magnetic stirring bar, into which 500 mL solution of 1 mM $AgNO_3$ was first loaded and then heated to boiling. Following that, a certain volume of 1% sodium nitrate solution was injected dropwise into the reactor. The resulting solution was stirred and maintained at 80 °C during the entire experiment by a thermally controlled magnetic stirrer. When the reaction solution turned orange-yellow, the AgNPs preparation was complete. To select optimal conditions for the AgNPs preparation, the effect of various process variables such as the mass ratio of reactants and boiled time was investigated.

Preparation of AgNPs@AC

The production of AgNPs@AC derived from rice husk was depicted in Fig. 1. Accordingly, the AC obtained from the rice husk carbonization was impregnated in the AgNPs solution and

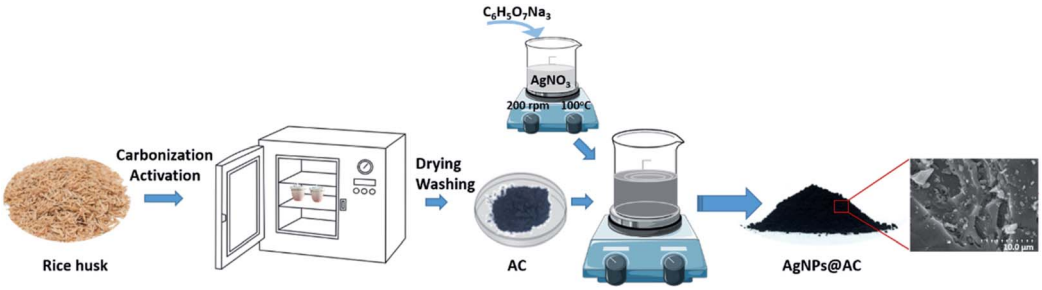

Fig. 1 Schema of the preparation of AgNPs@AC.

stirred continuously at room conditions for 4–12 hours. The mixture was then filtered *in vacuo* to remove filtrate and dried overnight at 110 °C. The concentration of AgNPs and stirring speed were also investigated in order to provide the optimal conditions for AgNPs@AC preparation. The obtained AgNPs@AC was analyzed for physicochemical properties before being used for floodwater treatment. As can be seen, the preparation method of AgNPs@AC described above is extremely simple and easy to perform. Thus, it is very suitable for the Vietnamese Mekong Delta where essential equipment is still lacking.

Characterization of AgNPs@AC

The morphology of as-synthesized AgNPs@AC was determined by scanning electron microscope (SEM, JSM-7800F, Jeol Ltd.; Tokyo, Japan) and transmission electron microscopy (TEM, Hitachi-HT7700, Hitachinaka, Japan). The crystalline structure of the sample was investigated using X-ray diffraction (XRD) on a Burker AXS D8 (Karlsruhe, Germany) diffractometer. The surface groups were identified by Fourier transform infrared (FTIR) spectrometer (Nicolet IS10, Thermo Fisher Scientific, USA). The specific surface area was calculated by the Brunauer–Emmett–Teller (BET) method (TriStar II 3020, Micromeritics, USA). Dynamic light scattering (DLS, SZ-100Z2, Horiba, Japan) measurements were used to examine the particle size distribution. The PerkinElmer NexIon 300D (Waltham, MA, US) was used to measure the concentration of AgNPs using inductively coupled plasma-mass spectrometry (ICP-MS).

Treatment of floodwater using AgNPs@AC

A simple filter system based on AgNPs@AC prepared under optimal conditions was developed for treating floodwater in the Mekong Delta region (Fig. 2). Before being discharged into the filtration column, the initial water source taken at Hau Giang River would be pre-treated by the coagulation method to preliminarily remove the suspended solids. Polyaluminum chloride (PAC) and kali alum were used in the coagulation process at the dosage ranging from 4 to 30 mg L^{-1}. The coagulant-added floodwater was stirred evenly for 5 minutes, and the sedimentation process lasted 30 min. After that, the pre-treated floodwater was passed through a filter column with a diameter of 60 mm from top to bottom. The thickness of the AgNPs@AC layer in the filter column was varied from 5 to 50 mm. A thin layer of quartz sand was placed on top of the AgNPs@AC layer to remove untreated suspended solids while also reducing the vortex speed of the water flowing through the AC layer. During the treatment process, the influent flow rate was kept constant at 50 mL min^{-1}.

The quality indicators of floodwater before and after treatment, including pH, turbidity, total dissolved solids (TDS), suspended solids (SS), and color, were measured using pH meter (Inolab Multi 9310 IDS, Germany), turbidity meter (Hach 2100Q, Loveland, CO, US), TDS meter (Hach HQ411d, Loveland, CO, US) and colorimeter (Spectroquant Move 100, Merck KgaA, Germany), respectively. The most probable number (MPN) method was used to detect total coliform and fecal coliform. All determinations were performed in triplicate in two separated experiments, and the average values were presented as final results. The relative error of the measurement varied between 1 and 3%.

Water quality indicators were also compared with standard values recommended by the World Health Organization (WHO) and by the National Technical Regulation on Domestic Water Quality of Vietnam (QCVN 01: 2009/BYT).

Results and discussion

Effect of carbonization and activation temperature on AC formation

The adsorption capacity of AC primarily depends upon surface area and micropore volume, which are controlled by carbonization and activation temperature. To assess the adsorption capacity of AC employed in wastewater treatment, various adsorbates such as methylene blue (MB), iodine (I), and phenols (Ph) are commonly used.[24,25] Although not providing any insight into the intrinsic properties of AC, the obtained outcome of these tests gives a technical estimate of the adsorption capacity of the studied material. A series of experiments were performed in this study to investigate the effects of various carbonization temperatures (400, 500, and 600 °C) on the adsorption capacity of AC derived from rice husk with activation time of 60 min at the activation temperatures ranging from 700 to 900 °C. Since phenol is highly toxic, methylene blue and iodine were used as the adsorbates to evaluate preliminarily the adsorption capacity of AC. The adsorption process was carried out under conditions similar to the floodwater treatment in order to obtain the most optimal AC suitable for this treatment. The adsorption abilities

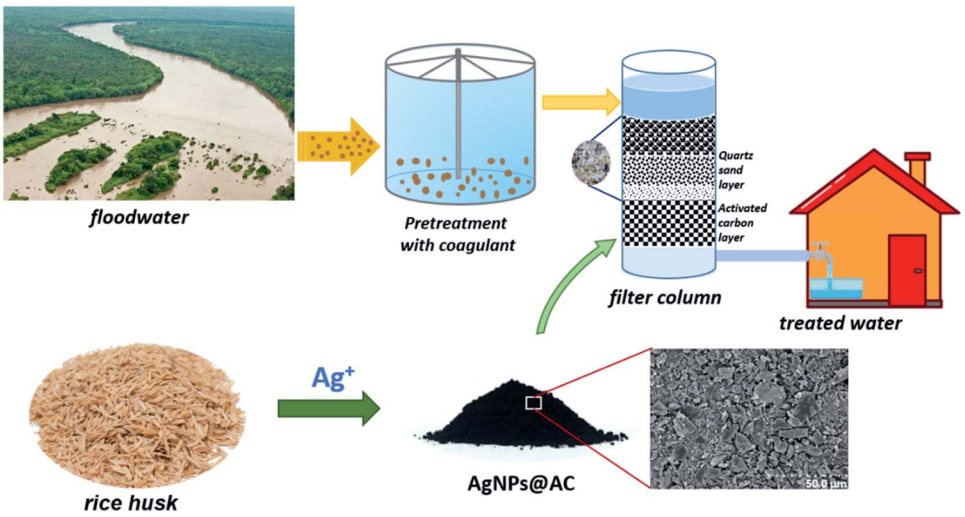

Fig. 2 Schema of floodwater treatment using AgNPs@AC.

of MB and I onto obtained AC were calculated by the following equation:

$$\text{Adsorption capacity } \left(\text{mg g}^{-1}\right) = \frac{C_0 - C_e}{m} \times V \qquad (1)$$

where C_0, C_e – the initial and equilibrium concentrations of MB or I (mg L^{-1}), respectively; V – the volumes of MB or I aqueous solution (L), and m – the mass of AC samples used (g).

Fig. 3 depicts an overview of the adsorption ability of MB and I onto AC derived from rice husk under different activation and carbonization temperatures. First of all, it can be clearly seen that the AC had a much higher iodine adsorption capacity than methylene blue. This phenomenon is most likely due to the presence of oxygen-containing surface groups in the AC structure, which enhances coating-substrate adhesion. Fig. 3 also reveals that there has been a sharp increase in the adsorption performance of AC at the activation temperature of 900 °C. This effect can be explained by the large number of pores produced at this temperature. Perhaps 900 °C is the optimal temperature for activating the carbon derived from plant wastes as many publications have proven before.[26–32] At the low temperature (600, 800 °C) the AC typically has very few pores. When the activation temperature is raised, the defects as well as roughness gradually begin to emerge, thereby resulting the slit-shaped cracks in the material surface. Through these cracks, the CO_2 can effortlessly diffuse into the inner material, which further accelerates the activation rate and the pore formation. Another interesting finding from this figure was that increasing the carbonization temperature in the standard range (400–600 °C) did not significantly increase the methylene blue and iodine adsorption capacity of the investigated material. From the foregoing, the activated carbon obtained by carbonizing and activating rice husk at 500 and 900 °C respectively was used for coating AgNPs. The particle size of the obtained AC was uniformly distributed in the range of 450 μm to 1300 μm (Fig. S1†), with only a very small number of AC particles having a size less than 100 μm. The special surface area of AC obtained under the above optimal preparation conditions was 810.023 m^2 g^{-1}. This value was significantly higher than that of rice husk activated by chemical as well as physical methods in the many previous studies.[29,31,33–35]

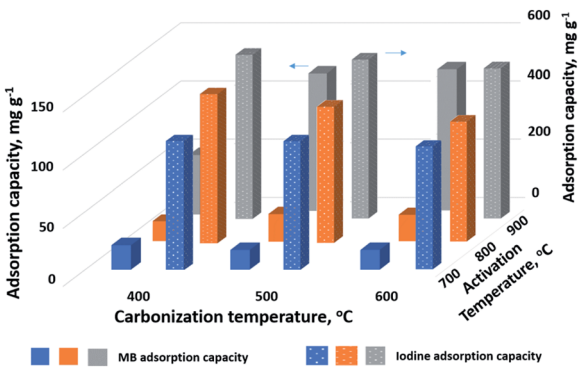

Fig. 3 Effect of carbonization and activation temperature on AC formation.

Effect of reagent dosage and reaction time on AgNPs formation

Prior to coating the silver onto the AC, the conditions for AgNPs solution formation must be optimized. Among the various parameters influencing AgNPs formation, the reagent dosage and reaction time are the most important factors towards AgNPS properties. Taking this into account, an investigation into the effect of two factors on AgNPs formation was performed, and the DLS method was employed to approximate the size distribution of AgNPs in the obtained solution.

Three propositions of $C_6H_5O_7Na_3$ to $AgNO_3$ ratios of 0.5 : 1, 1 : 1, and 2 : 1 were used to investigate the effect of reagent dosage on AgNPs formation at 80 °C. Preliminary results showed that at the low mass ratio (0.5 : 1), the reaction solution was almost colorless during the first 30 min of AgNPs synthesis,

and the DLS measurement outcome hardly was undetermined. The interesting finding could possibly be due to the low $C_6H_5O_7Na_3$ concentration being insufficient for the silver ion reduction. The color of the reaction solution changed to yellowish-brown after increasing the reagent dosage ratio to 1 : 1, indicating an amount of silver ions converted to nanoparticles. According to the particle size distribution analysis, the silver nanoparticles ranged in size from 44 to greater than 150 nm, were primarily concentrated at 63.3 nm, and then tended to reach equilibrium (Fig. S2a†). It can also be clearly seen that the continued increase in the amount of $C_6H_5O_7Na_3$ had no effect on the size of the AgNPs. In the other words, the reagent dosage ratio of 1 : 1 was optimal for the preparation of AgNPs.

In addition to the reagent dosage ratio, synthetic time is another important factor in determining the particle size of AgNPs. The size distribution histogram of AgNPs synthesized at the different reaction times (20, 30, 40, 60, and 90 min) revealed that, under otherwise uniform conditions, increasing the synthesis time expanded the particle-size distribution of AgNPs (Fig. S2b†). With regards to the biological aspect, AgNPs were discovered to have antibacterial effects at low concentrations. Furthermore, smaller-sized AgNPs were more effective against harmful microorganisms.[36,37] On the global market today, antimicrobial products frequently prioritize the use of silver nanoparticles with sizes ranging from 45–75 nm. Thus, AgNPs synthesized in the first 30 min would be used to coat AC derived from rice husk.

The final critical step in preparing the floodwater treatment material is to coat AgNPs onto AC. This procedure was carried out at the ambient condition using the impregnation method with varying AgNPs solution concentrations and reaction times. In Fig. S3,† there is a clear trend of increasing the content of AgNPs coated on AC by enhancing AgNPs solution concentration and stirring time. Nonetheless, this increase was not significant when AgNPs concentration was greater than 0.1 mg L^{-1} and stirring time was extended to 8 hours, indicating that the AgNPs on the AC surface had been saturated. Hence, the AgNPs@AC sample obtained optimally under such conditions was used to treat the floodwater in the Mekong Delta.

Characterization of AgNPs@AC

The resulting AgNPs@AC were characterized by XRD, FTIR spectroscopy, SEM, and TEM. Fig. 4a and b illustrated the morphology of the AgNPs@AC sample and the sizes distribution of AgNPs with dissimilar sizes in the range of 50–100 nm. What stands out in these figures is the even distribution of anisotropic silver nanoparticles on the surface as well as in the pores of AC. In addition to size, the shape of nanoparticles has a direct influence on their antibacterial properties.[38,39] In fact, it has been proven that anisotropic AgNPs contained mainly {111} lattice planes that acted as the maximum reactivity sites and, consequently, the antibacterial effectiveness of anisotropic AgNPs was higher than that of silver nanospheres or nanorods.[38,40,41]

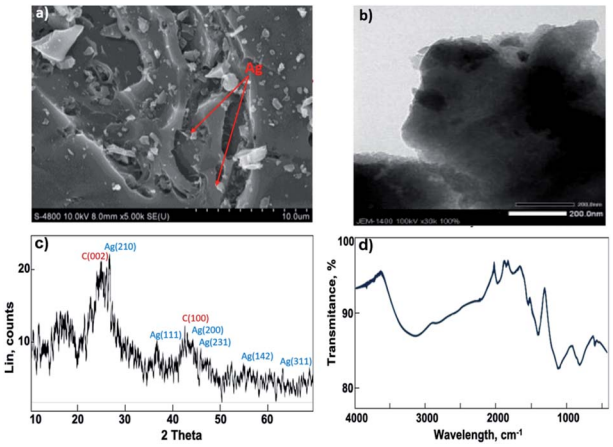

Fig. 4 SEM (a) image, TEM (b) image, XRD (c) and FTIR (d) spectrum of AgNPs@AC.

The X-ray diffraction pattern of the investigated material was shown in Fig. 4c. Two diffraction peaks at 2θ of 24 and 43.3° can be indexed to (002) and (100) diffraction for graphite carbon, respectively (JCPDS no. 75-1621). Several reflection peaks detected at 2θ of 27.4°, 37.5°, 44.3°, 46.21°, 54.83°, and 63.8° corresponded to the (210), (111), (200), (231), (142), and (220) crystal planes of the AgNPs structure, respectively (JCPDS no. 04-0783).[42,43] The coexistence of AC and AgNPs peaks in the XRD pattern of AgNPs@AC showed the stability of AgNPs on AC. The FTIR spectrum of AgNPs@AC used to identify its various functional groups was presented in Fig. 4d. The broad band at 3100–3400 cm^{-1} is assigned to –OH stretching vibration in the AgNPs@AC sample.[44] The adsorption bands located at 2800–2900 cm^{-1} and 1425 cm^{-1} were characterized for C–H bending vibration of CH_3, CH_2 groups.[45,46] The adsorption peaks at 1740, 1097, and 810 cm^{-1} were attributed to C=O stretching vibration group of the ester functional group, C–O and C–H bending of aromatic rings, respectively.[47] The resulting FTIR has demonstrated the presence of oxygen-containing surface groups in the AgNPs@AC structure, thereby explaining why the AC-derived rice huck possessed a much higher iodine adsorption capacity than methylene blue. Thus, the above-aforementioned characteristics of the AgNPs@AC sample promise to provide a superior material for the treatment of floodwater.

Treatment of floodwater using a filter system based on AgNPs@AC

Before going into treatment, a survey was conducted to assess the indicators of water quality in the flooded areas. The river water investigated in this study was primarily collected from eight different locations along the Hau Giang River in three provinces of the Vietnamese Mekong Delta. Each location is approximately 30 km apart on average, corresponding to a total survey length of more than 210 km extending from upstream to downstream of the Hau Giang River (Fig. 5). The water samples were taken before, during, and after the flood corresponding to July, September, and October of 2020. The sampling at these eight locations was carried out on the same day to obtain the

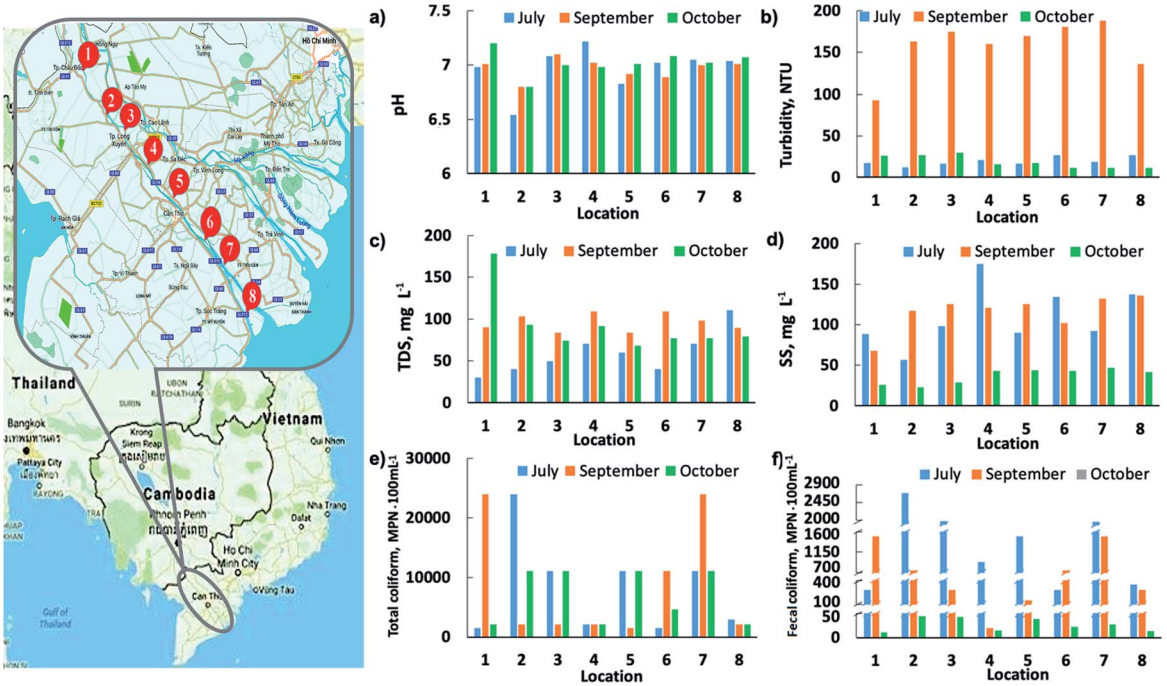

Fig. 5 The sampling locations along the Hau Giang River and preliminary survey of floodwater quality indicators in these locations.

most accurate comparisons. At each location, the samples were taken using sterilized 1.5 liter glass bottles at a depth of 30 cm below the water surface. Following the completion of sampling, all samples were immediately placed in an icebox for preservation while awaiting analysis. Within 24 hours of sample collection, biological indicators of water quality were analyzed. The following are detailed descriptions of the eight sampling locations:

- Location 1 (10°40′38.8″N 105°12′19.1″E): Khanh Hoa Commune, Châu Phú District, An Giang Province, Vietnam;

- Location 2 (10°27′45.4″N 105°20′59.4″E): Bình Thành Commune, Châu Thành District, Angiang Province, Vietnam;

- Location 3 (10°24′24.4″N 105°25′37.8″E): MyHoarding islet, Long Xuyên, Angiang Province, Vietnam;

- Location 4 (10°14′49.0″N 105°35′09.8″E): Tan Loc ward, Thót Nót District, Can Tho City, Vietnam;

- Location 5 (10°05′12.0″N 105°45′03.1″E): Conson, Bui Huu Nghia ward, Bình Thành District, Can Tho City, Vietnam;

- Location 6 (9°53′43.8″N 105°56′46.8″E): Phongmam Commune, Kê Sách District, Soc Trang Province, Vietnam;

- Location 7 (9°47′15.9″N 106°02′35.2″E): My Phuoc islet, Nhonmy Commune, Kê Sách District, Soc Trang Province, Vietnam;

- Location 8 (9°35′59.1″N 106°10′36.5″E): Daian 1 Commune, Cù Lao Dung District, Soc Trang Province, Vietnam.

Water quality characteristics at eight sampling locations were evaluated through several important parameters, such as pH, turbidity, TDS, SS, total coliform, and fecal coliform. As can be seen from Fig. 5, the pH value of river water before and after the flood period has been almost unchanged along the river, fluctuating in the range of 6.6–7.3. This figure also revealed a clear trend in which turbidity, TDS, and SS of the river water rapidly increased, peaking during flood season. This phenomenon is probably due to the fact that when annual floodwater overflows from upstream, it carries silt, alluvium, and organic matter, thereby significantly increasing the turbidity, TDS, and SS of river water. On the other hand, the leaching process, as well as the deposition of substances after the flood season, significantly reduced the values of these indicators. Total coliform and fecal coliform are the most important quality indicators for domestic water. Water contaminated with coliform bacteria can cause a variety of dangerous diseases such as diarrhea, typhoid, jaundice, and dysentery. The actual survey results showed that the total coliform index was higher than 1000 MPN/100 mL at most of the sampling locations along the Hau Giang River, and in many places up to 25 000 MPN/100 mL such as Khanh Hoa commune in Châu Phú District, Bình Thành Commune in Châu Thành District district, and My Phuoc islet in Nhonmy Commune. Furthermore, the fecal coliform indicator at these locations was greater than 1500 MPN/100 mL, and even at Bình Thành Commune of Châu Thành District, it reached 11 000 MPN/100 mL. Interestingly, there is a clear trend of decreasing fecal coliform index from before to after flood seasons. The reductions in fecal coliform concentrations were attributed to its dilution or overall removal by floodwater runoff. These findings could imply that the water in the Hau Giang River has been contaminated by possible pathogenic microorganisms. Comparison of the water quality indicators collected at Hau Giang River with standard values recommended by the World Health Organization (WHO) and by the National Technical Regulation on Domestic Water Quality of Vietnam (QCVN 01: 2009/BYT) has been illustrated in Table

S1.† Overall, except for pH and TDS, all of the water quality indicators obtained exceed the permissible limits prescribed by WHO and QCVN 01: 2009/BYT, especially for biological indicators. Thus, using AgNPs@AC as the antimicrobial filter to treat the floodwater of the Hau Giang River is a reasonable direction. However, the high turbidity can seriously interfere with the disinfection efficiency of the filter material by providing protection for the microorganisms and stimulating their growth during water treatment.[48–50] As a result, the initial floodwater source from the Hau Giang River would be pre-treated by the coagulation–sedimentation method to remove the suspended solids before being discharged into the filter column containing AgNPs@AC.

Pre-treating floodwater using coagulation–sedimentation method

The Kali alum and polymerized forms of aluminum such as PAC are regarded as the low-cost universal coagulants that have found widespread use in industrial water treatment plants.[51,52] In recent years, PAC has been used increasingly owing to its lower cost, better coagulation/flocculation performance, and effectiveness across a wide pH range than the conventional coagulants.[53–56] However, the treatment efficiency of these coagulants is heavily dependent on the natural characteristics of the water to be treated. Therefore, the preliminary experiments to investigate the coagulation–sedimentation performances of kali alum and PAC were carried out to choose the most suitable one for pre-treatment of floodwater in the Hau Giang River, in which the basic quality indicators of the floodwater were evaluated through the change in the concentration of these coagulants over a 10 min settling time. The obtained results, as shown in Fig. S4,† indicated that, with the exception of pH and total dissolved solids, other basic quality indicators of the floodwater were significantly reduced after undergoing coagulation–sedimentation. It is also clear that in all concentrations tested, PAC outperformed kali alum in terms of treatment efficiency. Thus, PAC obviously was chosen as an effective coagulant for the pre-treatment of floodwater. In addition to the coagulant type and natural characteristics of water, processing parameters such as coagulant dosage and settling time have an impact on coagulation–sedimentation performance.[57] Therefore, in order to achieve the best conditions for floodwater pre-treatment, the jar test was run in a batch mode with different process parameters such as PAC dosage and settling time. The most obvious finding to emerge from the analysis is that increasing the PAC dosage and settling time had almost no effect on the biological and physical-chemical indicator such as pH value (Fig. 6). In addition, the other indicators decreased rapidly within the first 20 min of settling and then remained nearly unchanged as the settling time increased. It is also important that when the PAC dosage raised from 20 mg L^{-1}, the turbidity and color removal rates increased, yielding maximum removal efficiencies of 90.52 and 83.73% after a settling time of 20 min, respectively. This correlation may partly be explained by an increase in the concentrations of hydrolysed aluminum species which destabilize the colloidal particles presenting in the floodwater. Excessive amounts of coagulant dosage can result in redispersion of colloidal particles.[58] As a result of the increased PAC dosage, the turbidity and color removal efficiencies were slightly reduced. One intriguing finding was that increasing the coagulant dosage above 20 mg L^{-1} did not only not reduce the TDS index in the floodwater, but actually increased it. This is understandable due to an excessive rise in the concentration of a solute called PAC. Particularly for the SS indicator, the reduction was proportional to the PAC dosage. After a 20 min settling time, the SS in the floodwater was almost completely removed by adding PAC at a dosage of 20 mg L^{-1}.

In general, the PAC dosage of 20 mg L^{-1} and settling time of 20 min are optimal for coagulation–sedimentation used in the pre-treatment of the floodwater. All floodwater quality indicators, with exception of color and biological parameters, meet standard requirements of WHO and QCVN 01: 2009/BYT for drinking water after the pre-treatment process.

Post-treating floodwater using AgNPs@AC. Using AgNPs@AC as an antimicrobial filter for the post-treatment of floodwater promises to improve its quality in terms of biological indicators. Indeed, even though the minimum height of the surveyed AgNPs@AC layer was only 5 mm, total coliforms and fecal coliforms in the floodwater were completely undetectable after posttreatment (Fig. 7). This proved that the AgNPs present in the AgNPs@AC layer easily destroyed the cell wall structure of microorganisms. Concurrently, the turbidity, TDS, SS, and color in treated water also remarkably decreased in comparison with the pre-treated one. This can be explained by the excellent adsorption ability of AgNPs@AC, which has a porous structure, large special surface area (697.74 m^2 g^{-1}), and numerous functional groups (–OH, –COOH, C=O). In addition, the pH value of the floodwater barely changed when it passed through the filter column.

However, a common issue encountered when using the AgNPs@AC layer for post-treatment of floodwater was that the inlet flow of floodwater could disturb the AgNPs@AC layer, leading to a serious impact on the outlet water quality. To address this challenge, we used a layer of quartz sand placed on top of the AgNPs@AC layer to prevent the water flow from directly impacting the activated carbon layer. Moreover, quartz sand is also a well-known traditional natural adsorbent that is widely employed as a substrate in water treatment.[59] Thus, one question was whether or not quartz sand could improve the quality of floodwater. In order to elucidate the unanswered question, we have conducted a series of independent experiments to evaluate the quality indicators of pre-treated floodwater before and after passing through the quartz sand layer. To obtain the most objective results, the influence of particle size of quartz sand and thicknesses of quartz sand layer on the floodwater treatment was also studied. The obtained outcome revealed that quartz sand did not clearly perform the role of an adsorbent in floodwater treatment (Fig. S5†). The most important insight gained from this study was to provide us with optimal thicknesses of quartz sand corresponding to each its particle size. Based on this result, we created a filter column composed essentially of vertically arranged component layers as follows: 20 mm quartz sand layer with the size of 2–3 mm;

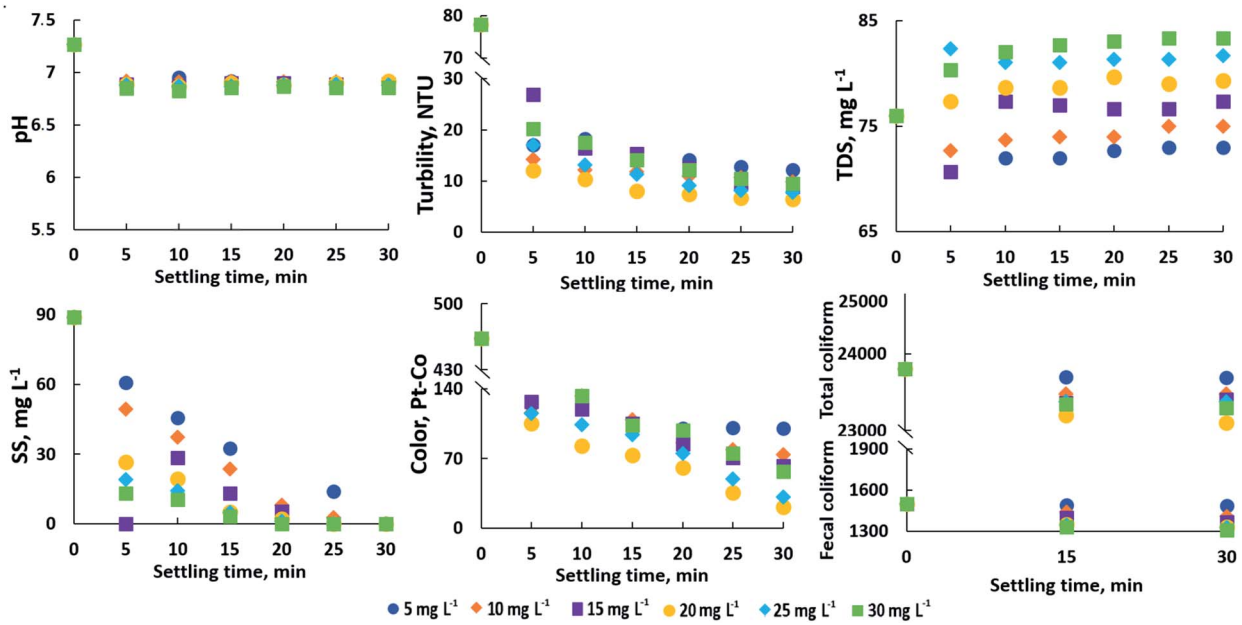

Fig. 6 Effect of PAC concentration and settling time on floodwater pre-treatment.

20 mm quartz sand layer with the size of 1–2 mm; 10 mm quartz sand layer with size 0.8–1 mm; and the AgNPs@AC layer.

The AgNPs@AC layer thickness is also one of the most important parameters to be considered. Preliminary survey results (Fig. 7) revealed the fact that the AgNPs@AC layer thickness has little effect on the quality of the outlet water. Interestingly, the suspended solid and color index were entirely eliminated when the pre-treated floodwater flowed through the filter column filled with AgNPs@AC and sand layer. It seems possible that this result is due to an increase in the blockage of suspended solids in the porous medium when the ratio of solid size and porous medium becomes bigger.[60] Overall, the floodwater that has been treated by the proposed filter system can be completely used to serve basic human needs.

Investigation of the service life of filter column

Eventually, the service life of the filter column is what we care about since it determines the practical significance of the filter system. The quality indicators (except biological) of floodwater

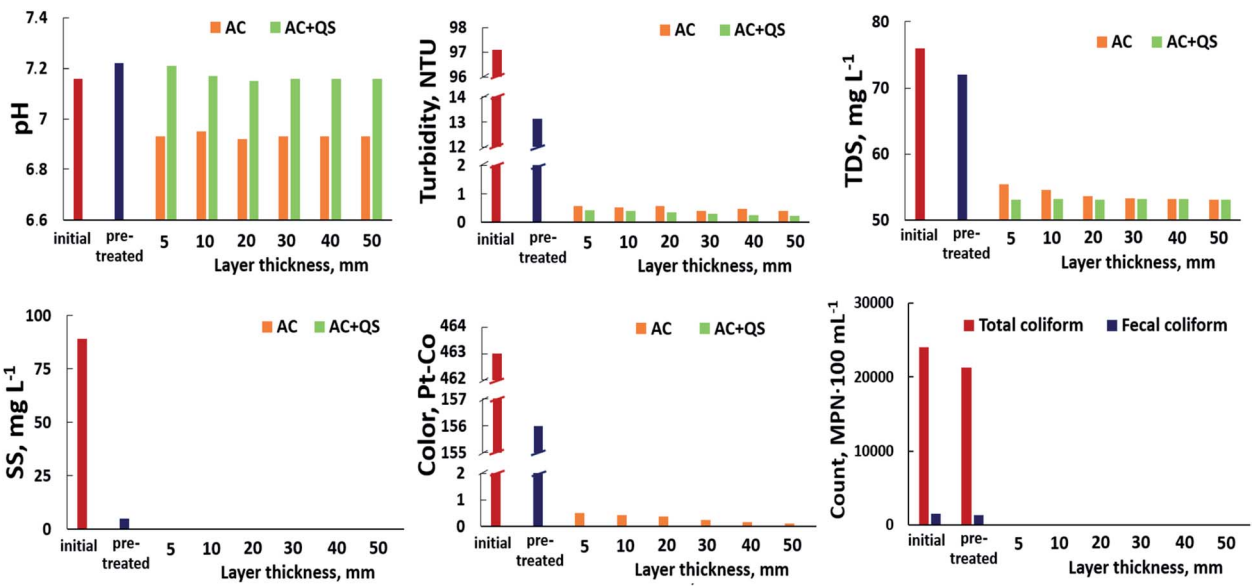

Fig. 7 Effect of the thickness of AgNPs@AC and AgNPs@AC + sand layer on floodwater treatment.

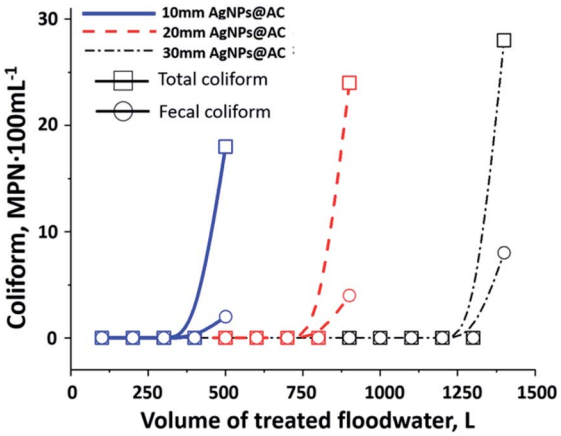

Fig. 8 The treatment capacity of the filter column based on AgNPs@AC.

after preliminary treatment by PAC mostly meet the standard requirements of WHO and QCVN 01: 2009/BYT. The service life of the filter column was therefore controlled by its antimicrobial activity which was a function of the thickness of the AgNPs@AC layer. With a processing capacity of 20 liters per day, the filter column comprised of 10 mm thick AgNPs@AC layer could continuously process 360 liters of the floodwater over the course of 18 working days (Fig. 8). The filter column lasted between 40 and 65 days when the thickness of the AgNPs@AC layer increased to 20 and 30 mm, respectively. Overall, on average per centimeter of the AgNPs@AC layer, the filter system can handle 410 liters of floodwater for more than 20 days. According to preliminary calculations (Table S2†), the treatment of one cubic meter of the floodwater using silver nanoparticles coated onto activated carbon will cost nearly 0.17$.

Conclusions

In summary, we have developed a simple and highly efficient filter system based on AgNPs@AC for the treatment of floodwater from the Hau Giang River. The filter layer consisted of AgNPs@AC was successfully prepared from rice husk and silver ions. The morphology of the as-synthesized AgNPs@AC was characterized using a scanning electron microscope (SEM), transmission electron microscope (TEM), X-ray diffraction (XRD), and Fourier transform infrared (FTIR) spectrometer. It has been demonstrated that after the pre-treatment process, all of the floodwater quality indicators met the standard requirements of the World Health Organization and the National Technical Regulation on Domestic Water Quality of Vietnam for drinking water. The obtained results clearly indicated that polyaluminum chloride exhibited an effective coagulant for floodwater pre-treatment in the Hau Giang River. The study has also shown that while the thickness of the AgNPs@AC layer had little effect on the outlet water quality, it completely determined the service life of the filter system. Taken together, these findings have confirmed the possibility of widespread and sustainable application of AgNPs@AC in the treatment of floodwater.

Author contributions

My Uyen Dao: writing – original draft, software, data curation, methodology, conceptualization. Anh Khoa Tran: project administration, data curation. Hong Hanh Cong: software, methodology. H. Y. Hoang: supervision, writing – original draft, writing – review & editing, software, data curation, methodology, validation.

Conflicts of interest

The authors declare that they have no known competing financial interests or personal relationships that could have appeared to influence the work reported in this paper.

References

1 E. Park, H. L. Ho, D. D. Tran, X. Yang, E. Alcantara, E. Merino and V. H. Son, *Sci. Total Environ.*, 2020, **723**, 138066.
2 F. O. Okaka and B. D. O. Odhiambo, *J. Environ. Public Health*, 2018, **2018**, 1–8.
3 Q. Liang, Y. Liu, M. Chen, L. Ma, B. Yang, L. Li and Q. Liu, *Mater. Chem. Phys.*, 2020, **241**, 122327.
4 D. N. K. P. Negara, T. G. T. Nindhia, I. W. Surata, F. Hidajat and M. Sucipta, *Mater. Today: Proc.*, 2020, **22**, 148–155.
5 K. G. Akpomie and J. Conradie, *Environ. Chem. Lett.*, 2020, **18**, 1085–1112.
6 V. T. Le, M. U. Dao, H. S. Le, D. L. Tran, V. D. Doan and H. T. Nguyen, *Environ. Technol.*, 2020, **41**, 2817–2832.
7 R. Nedjai, M. Alkhatib, N. Kabbashi, M. Z. Alam and N. Ahmed Kabbashi, *J. Environ. Treat. Tech.*, 2021, **9**, 686–697.
8 D. Vaddi, V. Mushini and P. S. Muralikrishna Mudumba, *J. Environ. Treat. Tech.*, 2021, **9**, 480–490.
9 M. U. Dao, H. S. Le, H. Y. Hoang, V. A. Tran, V. D. Doan, T. T. N. Le, A. Sirotkin and V. T. Le, *Environ. Res.*, 2021, **198**, 110481.
10 M. U. Dao, A. S. Sirotkin, V. T. Le, H. H. Cong, H. C. Nguyen and H. Y. Hoang, *Chem. Chem. Technol.*, 2021, **64**, 71–78.
11 A. Kheddo, L. Rhyman, M. I. Elzagheid, P. Jeetah and P. Ramasami, *SN Appl. Sci.*, 2020, **2**, 2170.
12 Y. Li, X. Zhang, R. Yang, G. Li and C. Hu, *RSC Adv.*, 2015, **5**, 32626–32636.
13 E. Menya, P. W. Olupot, H. Storz, M. Lubwama and Y. Kiros, *Biomass Convers. Biorefin.*, 2020, DOI: 10.1007/s13399-020-01158-2.
14 Z. Liu, Y. Sun, X. Xu, J. Qu and B. Qu, *ACS Omega*, 2020, **5**, 29231–29242.
15 S. Zafar, M. I. Khan, M. H. Lashari, M. Khraisheh, F. Almomani, M. L. Mirza and N. Khalid, *Emergent Mater.*, 2020, **3**, 857–870.
16 Y. Qing, L. Cheng, R. Li, G. Liu, Y. Zhang, X. Tang, J. Wang, H. Liu and Y. Qin, *Int. J. Nanomed.*, 2018, **13**, 3311–3327.
17 Y. Yang, T. Zhao and T. Zhang, *RSC Adv.*, 2021, **11**, 29519–29526.

18 A. Chauhan, R. Verma, S. Kumari, A. Sharma, P. Shandilya, X. Li, K. M. Batoo, A. Imran, S. Kulshrestha and R. Kumar, *Sci. Rep.*, 2020, **10**, 7881.
19 R. Salomoni, P. Léo, A. Montemor, B. Rinaldi and M. Rodrigues, *Nanotechnol., Sci. Appl.*, 2017, **10**, 115–121.
20 T. B. Devi, D. Mohanta and M. Ahmaruzzaman, *J. Ind. Eng. Chem.*, 2019, **76**, 160–172.
21 J. Turkevich, *Gold Bull.*, 1985, **18**, 86–91.
22 J. Turkevich and G. Kim, *Science*, 1970, **169**, 873–879.
23 M. Brust, M. Walker, D. Bethell, D. J. Schiffrin and R. Whyman, *J. Chem. Soc., Chem. Commun.*, 1994, 801–802.
24 C. Patawat, K. Silakate, S. Chuan-Udom, N. Supanchaiyamat, A. J. Hunt and Y. Ngernyen, *RSC Adv.*, 2020, **10**, 21082–21091.
25 H. Li, L. Liu, J. Cui, J. Cui, F. Wang and F. Zhang, *RSC Adv.*, 2020, **10**, 14262–14273.
26 X. Lan, X. Jiang, Y. Song, X. Jing and X. Xing, *Green Process. Synth.*, 2019, **8**, 837–845.
27 Y. X. Gan, *C*, 2021, **7**, 39.
28 W. Li, K. Yang, J. Peng, L. Zhang, S. Guo and H. Xia, *Ind. Crops Prod.*, 2008, **28**, 190–198.
29 M. Ahiduzzaman and A. K. M. Sadrul Islam, *SpringerPlus*, 2016, **5**, 1248.
30 L. Shrestha, M. Thapa, R. Shrestha, S. Maji, R. Pradhananga and K. Ariga, *C*, 2019, **5**, 10.
31 A. H. Wazir, I. U. Wazir and A. M. Wazir, *Energy Sources, Part A*, 2020, 1–11.
32 F. Rodríguez-Reinoso, M. Molina-Sabio and M. T. González, *Carbon*, 1995, **33**, 15–23.
33 S. Somasundaram, K. Sekar, V. K. Gupta and S. Ganesan, *J. Mol. Liq.*, 2013, **177**, 416–425.
34 S. B. Daffalla, H. Mukhtar and M. S. Shaharun, *PLoS One*, 2020, **15**, e0243540.
35 M. J. Saad, C. H. Chia, S. Misran, S. Zakaria, M. S. Sajab and M. H. Abdul Rahman, *Sains Malays.*, 2020, **49**, 2261–2267.
36 C. Baker, A. Pradhan, L. Pakstis, D. Pochan and S. I. Shah, *J. Nanosci. Nanotechnol.*, 2005, **5**, 244–249.
37 I. X. Yin, J. Zhang, I. S. Zhao, M. L. Mei, Q. Li and C. H. Chu, *Int. J. Nanomed.*, 2020, **15**, 2555–2562.
38 M. Raza, Z. Kanwal, A. Rauf, A. Sabri, S. Riaz and S. Naseem, *Nanomaterials*, 2016, **6**, 74.
39 L. Wang, C. Hu and L. Shao, *Int. J. Nanomed.*, 2017, **12**, 1227–1249.
40 B. Sadeghi, F. S. Garmaroudi, M. Hashemi, H. R. Nezhad, A. Nasrollahi, S. Ardalan and S. Ardalan, *Adv. Powder Technol.*, 2012, **23**, 22–26.
41 P. Van Dong, C. H. Ha, L. T. Binh and J. Kasbohm, *Int. Nano Lett.*, 2012, **2**, 9.
42 T. K. M. Prashantha Kumar, T. R. Mandlimath, P. Sangeetha, P. Sakthivel, S. K. Revathi, S. K. Ashok Kumar and S. K. Sahoo, *RSC Adv.*, 2015, **5**, 108034–108043.
43 Y. Meng, *Nanomaterials*, 2015, **5**, 1124–1135.
44 S. Pal, R. Nisi, M. Stoppa and A. Licciulli, *ACS Omega*, 2017, **2**, 3632–3639.
45 L. Zhang, L. Tu, Y. Liang, Q. Chen, Z. Li, C. Li, Z. Wang and W. Li, *RSC Adv.*, 2018, **8**, 42280–42291.
46 Q. Cui, Y. Zheng, Q. Lin, W. Song, K. Qiao and S. Liu, *RSC Adv.*, 2014, **4**, 1630–1639.
47 S. M. Alshuiael and M. A. Al-Ghouti, *PLoS One*, 2020, **15**, e0232997.
48 O. Fatoki, N. Muyima and N. Lujiza, *Water SA*, 2001, **27**(4), 467–474.
49 A. K. Singh, B. Raj, A. K. Tiwari and M. K. Mahato, *Environ. Earth Sci.*, 2013, **70**, 1225–1247.
50 RS2, *Guidelines for drinking-water quality: fourth edition incorporating the first addendum*, World Health Organization, Geneva, 2017.
51 A. I. Zouboulis and N. Tzoupanos, *Desalination*, 2010, **250**, 339–344.
52 H. Cui, X. Huang, Z. Yu, P. Chen and X. Cao, *RSC Adv.*, 2020, **10**, 20231–20244.
53 Z. Wu, X. Zhang, J. Pang, J. Li, J. Li and P. Zhang, *RSC Adv.*, 2020, **10**, 7155–7162.
54 A. K. Choudhary, S. Kumar and C. Sharma, *Desalin. Water Treat.*, 2015, **53**, 697–708.
55 N. D. Tzoupanos, A. I. Zouboulis and C. A. Tsoleridis, *Colloids Surf., A*, 2009, **342**, 30–39.
56 Z. You, H. Xu, Y. Sun, S. Zhang and L. Zhang, *RSC Adv.*, 2018, **8**, 40639–40646.
57 V. M. Bhandari and V. V. Ranade, in *Industrial Wastewater Treatment, Recycling and Reuse*, Elsevier, 2014, pp. 81–140.
58 J. Bratby, *Coagulation and Flocculation in Water and Wastewater Treatment*, IWA Publishing, 3rd edn, 2016.
59 C. Jiang, L. Jia, B. Zhang, Y. He and G. Kirumba, *J. Environ. Sci.*, 2014, **26**, 466–477.
60 J. Hou, X. Xu, L. Lan, L. Miao, Y. Xu, G. You and Z. Liu, *Environ. Pollut.*, 2020, **263**, 114499.